Published in final edited form as:

Neuroscience. 2014 September 5; 275: 519–530. doi:10.1016/j.neuroscience.2014.06.033.

MATCHING OF FEEDBACK INHIBITION WITH EXCITATION ENSURES FIDELITY OF INFORMATION FLOW IN THE ANTERIOR PIRIFORM CORTEX

D. C. SHERIDAN[a], **A. R. HUGHES**[b], **F. ERDÉLYI**[c], **G. SZABÓ**[c], **S. T. HENTGES**[b], and **N. E. SCHOPPA**[a,*]

D. C. SHERIDAN: dsheridan@regis.edu; G. SZABÓ: szabo.gabor@koki.mta.hu; S. T. HENTGES: Shane.Hentges@colostate.edu

[a]University of Colorado Anschutz Medical Campus, Department of Physiology & Biophysics, 12800 East 19th Avenue, Aurora, CO 80045, United States

[b]Department of Biomedical Sciences, Colorado State University, 1680 Campus Delivery, Fort Collins, CO 80523, United States

[c]Institute of Experimental Medicine, Division of Medical Gene Technology, Budapest, Hungary

Abstract

Odor-evoked responses in mitral cells of the olfactory bulb are characterized by prolonged patterns of action potential (spike) activity. If downstream neurons are to respond to each spike in these patterns, the duration of the excitatory response to one spike should be limited, enabling cells to respond to subsequent spikes. To test for such mechanisms, we performed patch-clamp recordings in slices of the mouse anterior piriform cortex. Mitral cell axons in the lateral olfactory tract (LOT) were stimulated electrically at different intensities and with various frequency patterns to mimic changing input conditions that the piriform cortex likely encounters *in vivo*. We found with cell-attached measurements that superficial pyramidal (SP) cells in layer 2 consistently responded to LOT stimulation across conditions with a limited number (1–2) of spikes per stimulus pulse. The key synaptic feature accounting for the limited spike number appeared to be somatic inhibition derived from layer 3 fast-spiking cells. This inhibition tracked the timing of the first spike in SP cells across conditions, which naturally limited the spike number to 1–2. These response features to LOT stimulation were, moreover, not unique to SP cells, also occurring in a population of fluorescently labeled interneurons in glutamic acid decarboxylase 65-eGFP mice. That these different cortical cells respond to incoming inputs with 1–2 spikes per stimulus may be especially critical for relaying bulbar information contained in synchronized oscillations at beta (15–30 Hz) or gamma

*Corresponding author. Address: Department of Physiology and Biophysics, University of Colorado School of Medicine, 12800 East 19th Avenue, Room P18-7115, Campus Box 8307, Aurora, CO 80045, United States. Tel: +1-303-724-4523; fax:+1-303-724-4501. Nathan.Schoppa@ucdenver.edu (N. E. Schoppa).

DISCLOSURES

The authors report that they have no conflict of interest associated with these studies.

Keywords

olfactory; gamma oscillations; piriform cortex; inhibition; mitral cell

INTRODUCTION

Cortical circuits are endowed with numerous sub-types of GABAergic interneurons that target both excitatory pyramidal cells, as well as other GABAergic cells. Within the primary olfactory, or piriform, cortex, several types of GABAergic interneurons have been identified based on their localization, anatomy, and biochemical properties (Ekstrand et al., 2001; Zhang et al., 2006; Young and Sun, 2009; Suzuki and Bekkers, 2010a,b; Bekkers and Suzuki, 2013). Targets of at least two of these cell-types in the anterior piriform cortex (aPC) have also been identified. GABAergic interneurons in layer Ia appear to provide inhibition on the dendrites of both superficial pyramidal (SP) cells located in layer 2 (L2) and another class of excitatory cells, the semilunar cells. In contrast, fast-spiking multipolar cells located in layer 3 (L3 FS cells) target inhibition onto the cell bodies of these same cells (Stokes and Isaacson, 2010; Suzuki and Bekkers, 2012).

At the level of action potential (spike) activity, somatic inhibition can profoundly impact the cortical response to mitral cell inputs arriving from the olfactory bulb. Following electrical stimulation of mitral cell axons in the lateral olfactory tract (LOT), this inhibition can shorten the duration of the evoked excitatory post-synaptic potential (EPSP) and spiking in superficial pyramidal cells (SP cells) (Tseng and Haberly, 1988; Luna and Schoppa, 2008). Inhibition acting to limit the duration of spiking has also been observed *in vivo*, during each cycle of odor-evoked gamma frequency (30–80 Hz) oscillations (Litaudon et al., 2008; Poo and Isaacson, 2009). Such a limited excitatory response could facilitate the SP cell response to prolonged incoming activity patterns from mitral cells (Margrie and Schaefer, 2003; Bathellier et al., 2008; Cury and Uchida, 2010; Patterson et al., 2013) that can include synchronized oscillations at the beta (15–30 Hz) or gamma (30–80 Hz) frequency (Adrian, 1950; Kashiwadani et al., 1999; Neville and Haberly, 2003; Martin et al., 2004; Beshel et al., 2007). A limited spike number following one round of input should allow SP cells to respond to subsequent inputs. It remains unclear, however, whether the ability of inhibition to limit spike number is robust. Such an effect of inhibition could be lost with different levels of LOT input, if inhibition and excitation scale differently with input strength from mitral cells, or during incoming stimulus patterns, if inhibition and excitation have differing short-term plasticity properties.

In this study, we performed patch-clamp recordings in slices of the mouse aPC to examine the impact of somatic inhibition on cortical responses while varying LOT stimulation intensity and stimulus patterns. Spike activity was recorded during cell-attached recordings, which was followed by whole-cell measurements of excitatory and inhibitory post-synaptic currents (EPSCs and IPSCs) to examine the mechanisms that shape the spike responses. Most recordings were in SP cells, but we also performed a subset of recordings in GFP-labeled cells in glutamic acid decarboxylase (GAD) 65-eGFP mice (Lopez-Bendito et al., 2004; Zhang et al., 2006). In both cell types, we found that a component of delayed

inhibition likely derived from L3 FS cells consistently limited the spike response to 1–2 spikes per stimulus pulse across varying stimulus conditions.

EXPERIMENTAL PROCEDURES

All experiments were approved by the Institutional Animal Care and Use Committee at the University of Colorado Anschutz Medical Campus, in accordance with National Institutes of Health (NIH) guidelines.

Brain slice preparation and electrophysiology

Sagittal slices (300 μm) were prepared from the aPC of postnatal day 8–28 transgenic mice (male and female) that were heterozygous for GAD65-eGFP (B6CBAF1/J background; Lopez-Bendito et al., 2004). The slicing procedure was modified from that previously reported for preparation of olfactory bulb slices (Schoppa et al., 1998). Briefly, mice were anaesthetized with isofluorane and euthanized by decapitation. Brains were excised and placed in an ice-cold solution consisting of (in mM) 83 NaCl, 72 sucrose, 26 $NaHCO_3$, 10 glucose, 3.5 KCl, 3 $MgCl_2$, 1.25 NaH_2PO_4, and 0.5 $CaCl_2$. Brain hemispheres were sliced separately with a VT1000S or VT1200S vibratome (Leica, Buffalo Grove, IL, USA). After slicing, cortical slices were incubated in a solution consisting of (in mM): 125 NaCl, 25 $NaHCO_3$, 1.25 NaH_2PO_4, 25 glucose, 3 KCl, 2 $MgCl_2$, 1 $CaCl_2$ (295 mOsm, pH 7.3 with 95% 0_2/5% CO_2 gas), and allowed to recover for 30–45 min at 33 °C. Brain slices were visualized with a 40× objective on an Axioskop 2 FS plus microscope (Carl Zeiss, Thornwood, NY, USA), equipped with differential interference contrast optics and an HBO 100 mercury lamp for fluorescence measurements. The aPC was identified based on its location relative to LOT and compact density of cells in L2. Experiments were conducted at 28 to 31 °C.

The base extracellular recording solution for the patch-clamp recordings contained (in mM): 125 NaCl, 25 $NaHCO_3$, 1.25 NaH_2PO_4, 25 glucose, 3 KCl, 0.5–1.0 $MgCl_2$, 2 $CaCl_2$ (295 mOsm, pH 7.3 with 95% 0_2/5% CO_2 gas). Except where noted, the $GABA_B$ receptor antagonist CGP55845 (2–4 μM) was also added to the bath to minimize presynaptic inhibitory effects on glutamate release from associational fibers (Tang and Hasselmo, 1994; Franks and Isaacson, 2005). In parallel recordings, done with and without CGP55845, we found that the drug had no effect on the basic spike response in SP cells (compare Fig. 3B with its inset) nor on the onset- or rise-times of IPSCs ($n = 7$; $p > 0.48$ for both parameters). The internal pipette solution for cell-attached recordings contained 150 mM NaCl. For whole-cell recordings of EPSCs and IPSCs at different LOT stimulus intensities (Fig. 2), the internal solution included: 140 Cs-gluconate, 10 phosphocreatine, 10 TEA-Cl, 5 HEPES, 1 EGTA, 1 MgATP (280 mOSM, pH 7.2 with CsOH), along with 5 mM QX314 to block sodium channel-dependent action potentials. For other whole-cell recordings, the pipette solution contained (in mM): 125 K-gluconate, 10 HEPES, 1 EGTA, 2 $MgCl_2$, 0.025 $CaCl_2$, 2 NaATP, 0.5 NaGTP, and 5 QX314 (215 mOsm, pH 7.3 with KOH). Current and voltage signals were recorded with a Multi-Clamp 700B dual patch-clamp amplifier (Molecular Devices, Sunnyvale, CA, USA), digitized at 10 kHz, and filtered at 2.5–4 kHz. Data were acquired and analyzed with Axograph X (Axograph Scientific). We generally excluded

whole-cell recordings from analysis if the test cells had resting membrane potentials more depolarized than −60 mV or if the series resistance during the recording obtained values of >20 MΩ.

Electrical stimulation was performed using a broken-tip patch pipette (4–6 μm) positioned directly on the LOT, always within 150 μm in the lateral direction with respect to the cell body of the test cells. A stimulus isolator (A365; World Precision Instruments, Sarasota, FL, USA) delivered single stimuli or stimulus patterns generated by a Macintosh G5 computer. Stimulus pulses/trains were delivered every 20–60 s to minimize current rundown. The stimulus intensity was varied between 10 and 200 μA, as indicated.

Most experiments involving a stimulus train applied to LOT were conducted at 100-μA intensity. The exceptions were the parallel recordings of IPSCs in SP cells and spiking in various classes of interneurons (Fig. 7C, D), which used weaker stimuli (30–80 μA). This was done in order to capture the complex facilitating-then-depressing dynamics of the IPSC response, which was to be compared to spikes in interneurons. Stimulus artifacts were blanked from the data traces in the figures.

For morphological analysis of SP cells and GAD65-eGGFP cells (Fig. 2A, Fig. 5A), 0.2% biocytin was included in the whole-cell patch pipette solution. Following fixation of slices in 4% formaldehyde, Cy5-conjugated streptavidin (1 μg/ml; Jackson ImmunoResearch, West Grove, PA, USA) was added. Cells were visualized under a confocal microscope (Olympus BX61WI FV1000 or the Olympus BX50 in the Rocky Mountain Taste and Smell Center at the University of Colorado Anschutz Medical Campus).

In the kinetic analysis of EPSCs and IPSCs, onset-times were estimated from the peak of the stimulation artifact to the point at which the current first deviated from baseline, as determined by eye. Onset-times for EPSCs were measured from the averaged current response. Analysis of IPSCs was based on individual stimulus trials.

Data values are reported as mean ± SEM. Paired or unpaired Student's *t* tests were most commonly used to determine statistical significance ($p < 0.05$; indicated with asterisks in figures). When comparisons were made across multiple stimulus intensities or stimulus train pulse number, ANOVA was followed by Tukey's HSD test.

Cell identification

For cell-attached recordings and initial cell-identification for whole-cell recordings, SP cells were distinguished based on cell body morphology (~20-μm-width, triangular), location in L2, and absence of fluorescence in GAD65-eGFP mice. Upon whole-cell recording, SP cell identity was confirmed by morphology (Fig. 2A) and input resistance values (mean = ~110 MΩ; see Table 1) that matched prior reports in mice (Suzuki and Bekkers, 2006). A few of our measures of responsiveness in SP cells differed from published reports. For example, our value for the action potential half-width (~1.7 ms) was larger than prior values (~0.8 ms; Suzuki and Bekkers, 2011). This likely was due at least in part to our relatively low recording temperature (28–31 °C) as compared to that prior study (33–35 °C). In separate experiments done at a higher temperature (32 °C), the action potential half-width in SP cells

was 1.2 ± 0.2 ms (n = 3). We also sometimes observed depressing EPSCs in response to a stimulus train applied to LOT (Fig. 4A), in contrast to prior reports of a facilitating profile (Stokes and Isaacson, 2010; Suzuki and Bekkers, 2011). This difference appeared to reflect the LOT stimulus intensity (see *Results*).

L2 GAD65-eGFP cells were identified based on their green fluorescence. For cell-attached recordings of spike activity in L3 FS cells, we selected cells with oblong cell bodies in L3. In parallel whole-cell current-clamp recordings, we confirmed that the cells identified based on location and cell body shape had the multipolar morphology and fast, non-accommodating spike behavior reported previously for L3 FS cells (Suzuki and Bekkers, 2010b; Stokes and Isaacson, 2010). Putative interneurons in L1 were identified based on their laminar location and round cell bodies (Suzuki and Bekkers, 2010b). Two of five L1a interneurons were also GFP-positive.

Fluorescent *in situ* hybridization and immunodetection of GFP

Preparation of brain slices and treatment procedures for studies with fluorescent anti-sense probes for vesicular glutamate transporters (VGLUT1 and VGLUT2) and immunodetection of GFP were similar to a previous report (Whitesell et al., 2013). A Cy5-conjugated antibody was used to detect GFP as the fluorescence was quenched during the *in situ* hybridization procedure. GAD65 was detected using 2 digoxigenin (DIG)-labeled probes to different regions of the mRNA simultaneously. To detect both GAD65 and glutamic acid decarboxylase 67 (GAD67) together, the tissue was first exposed to the DIG-labeled GAD67 probe overnight at 70 °C then to the DIG-labeled GAD65 probes at 52 °C overnight. The DIG-labeled probes were detected using a sheep-anti-DIG antibody conjugated to horseradish peroxidase (1:1000; Roche Applied Sciences) and visualized using TSA-biotin (Perkin Elmer, Waltham, MA, USA; per manufacturer's instructions) and streptavidin conjugated to Alexa-555 (1:1000; Life Technologies, Grand Island, NY, USA). Other details of the probes, specificity, and the complete procedure were previously described (Jarvie and Hentges, 2012). For clarity, the GFP signal (Cy5-fluorescence) and antisense probes (Alexa-555 fluorescence) are shown in Fig. 5E in green and red, respectively.

Sections were imaged on an Olympus Fluoview 1000 confocal microscope using 20× air and 40× oil immersion objectives. Autofluorescence was minimized by imaging the no-primary control slices and consecutively decreasing photomultiplier tube sensitivity until fluorescence could no longer be visually detected. Images were focused approximately 10 μm into the depth of the tissue and were acquired by sequentially scanning with individual lasers using a Kalman filter. Colocalization between GAD65-eGFP (assayed with GFP antibody) and the various antisense probes was assessed first by creating regions-of-interest that encircled cells with positive staining for GFP. We then calculated the percentage of cells that showed colocalization with the anti-sense probes. For each antisense probe, we collected regions-of-interest data from four to five slices from two different mice.

RESULTS

Inhibition ensures a low number of spikes in SP cells across variable LOT stimulus intensities

Prior studies in rat aPC slices provided evidence that GABAergic inputs onto SP cells can limit the response to single-shock stimulation of mitral cell axons in the LOT to about one spike per stimulus pulse (Luna and Schoppa, 2008). These prior recordings were done using relatively weak stimuli, when there were numerous spike failures, and our first objective was to assess whether the low spike number was consistently observed upon changes in LOT stimulus intensity.

During cell-attached recordings in mouse aPC slices (n = 21), we sampled both weak-to-moderate stimuli that were perithreshold for spiking in SP cells (~50% failure rate; mean intensity = 57 ± 4 μA) as well as stronger stimuli that resulted in spikes in every trial and with much shorter onset delays (Fig. 1A–C). Thus, our studies examined stimuli that caused quite variable circuit behaviors. However, as long as spikes were evoked in a given trial, all stimuli produced a similar, low number of spikes that ranged between 1 and 2 (Fig. 1A, D; no significant differences in comparisons between all stimulus intensities). The limited number of stimulus-evoked spikes appeared to result from GABAergic inhibition, since the $GABA_A$ receptor blocker gabazine (10 μM) greatly increased the spike number (Fig. 1D, E; n = 3); gabazine also increased spike probability in SP cells (from 0.3 ± 0.1 to 0.9 ± 0.1 at low-to-moderate stimulus intensities, n = 5; p = 0.031). These effects of gabazine appeared to be due to an augmented EPSP evoked by LOT stimulation (Luna and Schoppa, 2008), rather than changes in resting potential (control = −72 ± 1 mV, gabazine = −72 ± 1 mV; n = 3) or input resistance (control = 124 ± 18 MΩ, gabazine = 125 ± 24 MΩ; n = 6) of SP cells.

To understand how inhibition limited the SP cell spike response across LOT stimulus intensities, we recorded EPSCs and IPSCs (Fig. 2). EPSCs and IPSCs could be largely isolated in the same recording by adjusting the holding potential (−77 mV for EPSCs, −7 mV for IPSCs) and using a standard low-chloride pipette solution. Across a range of stimulus intensities similar to that assayed to measure spikes in Fig. 1, the isolated EPSCs always included a significant monosynaptic component (onset delays ≤ 2.5 ms; n = 16; Fig. 2A). The evoked IPSCs, in contrast, occurred with much longer onset-delays after the stimulus (mean onset-delay ≥ 7 ms for all intensities; Fig. 2A, B). An interesting feature of inhibition was that its onset-delay was consistently well-matched to that of spiking (Fig. 2B; no significant differences in all comparisons for given stimulus intensities), even though both delay values varied considerably with stimulus intensity. The matching in the timing of inhibition and spiking likely contributed to the maintenance of a low number of spikes, since if the SP cell spiked at all during a given trial, inhibition would naturally limit the spike number to near one.

We also observed a scaling in the amplitude of the evoked EPSCs and IPSCs, as assessed both in direct comparisons of EPSCs and IPSCs obtained in the same recording (Fig. 2C), as well as in plots of normalized current amplitude versus stimulus intensity (Fig. 2D; no significant differences in all comparisons for given stimulus intensities). A matching in the amplitude of excitation and inhibition should also promote a similar spike number across

stimulus intensity. In these recordings, the EPSCs likely reflected a mixed excitatory response that included both monosynaptic signals derived from mitral cell axons as well as recurrent excitation that was initiated by LOT stimulation. The stimulus intensity was often above ~60 μA, the average perithreshold intensity for spike activity in SP cells (see above). The recurrent excitation did not appear to reflect direct excitation of SP cells by the electrical stimuli, since SP cells displayed prolonged spike delays even at high LOT intensities (Fig. 1C).

Inhibition ensures a low number of spikes in SP cells during stimulus trains

We next assessed whether inhibition can promote a consistent, low spike number in SP cells during stimulus trains applied to LOT. Such stimuli should mimic the natural firing patterns of input mitral cells that can engage in inhalation-coupled spike bursts (Margrie and Schaefer, 2003; Cury and Uchida, 2010) as well as synchronized oscillations (Adrian, 1950). Analyzing five pulses of a 20-Hz stimulus train applied to LOT at a fixed intensity (100 μA), we found that SP cells consistently responded with an invariant and low number of stimulus-evoked spikes following each stimulus ($n = 7$; Fig 3A, B), similar to the single-shock experiments (Fig. 1). For the first stimulus pulse, the mean number of evoked spikes was near 2 (2.1 ± 0.4), but this value was not significantly higher than for pulse 2 (1.2 ± 0.1, $n = 7$; $p = 0.08$). GABAergic inhibition was responsible for maintaining the low spike number across the train, since gabazine (10 μM) increased spike number (Fig. 3A, B; $n = 7$, $p < 0.05$ for all stimulus numbers). Notably, the spike number across the train was insensitive to whether the $GABA_B$ receptor antagonist CGP55845 (2–4 μM) was added to the bath solution (compare the main plot in Fig. 3B with the inset). CGP55845 was included in most recordings throughout our study to minimize presynaptic inhibitory effects on glutamate release from associational fibers (Tang and Hasselmo, 1994; Franks and Isaacson, 2005; see *Experimental procedures* Section ‘Brain slice preparation and electrophysiology’).

Another clear feature of the response to 20-Hz stimuli, which was disrupted upon application of gabazine ($n = 6$), was a highly reproducible spike time across stimulus pulses (Fig. 3A, C; $p = 0.01$ in comparisons of the standard deviation of spike time, with and without gabazine; Pouille and Scanziani, 2001). The extra spikes observed in gabazine across the five stimuli likely reflected both additional spikes driven by each stimulus, as well as spikes that were carried over from prior stimuli (for stimulus pulses 2–5). Thus, inhibition helps to preserve both a precise number and timing of spikes for each pulse in a stimulus train.

Because mitral cell oscillations can vary in frequency between beta (15–30 Hz) and gamma (30–80 Hz) ranges (Adrian, 1950; Kashiwadani et al., 1999; Neville and Haberly, 2003; Martin et al., 2004; Beshel et al., 2007), we also examined the responses of SP cells to variable frequency stimulus trains. The responses to 10-, 40-, and 100-Hz trains (100 μA) were very similar to those following 20-Hz stimuli, with 1–2 spikes being evoked per stimulus ($n = 5$ for each frequency; Fig. 3D). At 100 Hz, there was one difference in the responsiveness across the train, as compared to lower frequency stimuli, which was that the probability that a given stimulus evoked a spike dropped across the train (Fig. 3E). This

effect could have reflected vesicle depletion at LOT-to-SP cell synapses or accumulating inhibition.

Could the near-constant spike response of SP cells across stimulus trains be explained by the properties of excitation and inhibition, as found above with changing LOT stimulus intensities (Fig. 2)? At the 100-μA stimulus intensity used for the spike measurements in Fig. 3, a close match was indeed observed in the onset-times of inhibition and spiking in SP cells across the stimulus train (n = 7 for each measurement; Fig. 4A, B), which should have limited the number of evoked spikes to near one. The amplitude of the IPSCs and EPSCs also scaled similarly with stimulus number, with both being depressing (Fig. 4A, C; n = 7). It should be noted that the depressing EPSCs in SP cells evoked by our 20-Hz LOT trains deviated from prior reports of facilitating monosynaptic EPSCs (Stokes and Isaacson, 2010; Suzuki and Bekkers, 2011). This likely reflected the fact that our trains employed relatively strong stimuli (100 μA) that recruited recurrent excitation (see above). In support of this conclusion, we found that EPSCs in SP cells following weaker LOT stimuli (40–50 μA) were facilitating (n = 3; data not shown).

Inhibition ensures a low number of spikes in a population of labeled cells in GAD65-eGFP mice

Our results thus far have indicated that inhibition limits the SP cell response to 1–2 spikes per stimulus for a variety of LOT stimulus conditions. To test whether a similar effect occurs in a population of interneurons, we recorded from GAD65-eGFP mice (Lopez-Bendito et al., 2004), which label a population of cells in L2 in both the aPC and posterior piriform cortex (Zhang et al., 2006). Within the posterior piriform cortex, L2 GAD65-eGFP cells immunostain for GABA and have a stereotyped morphology that is dominated by an ascending tufted dendritic tree and an axon that ramifies extensively in L2 and L3. These cells also display weakly adapting spiking in response to direct somatic current injections.

In our analysis, we first further characterized L2 GAD65-eGFP cells in the aPC. L2 GAD65-eGFP cells in this region had oblong or tear-drop-shaped cell bodies and, as in the posterior piriform cortex, a large, branching ascending dendrite (Fig. 5A; n = 7), axons that ramified extensively in L2 and L3 (in two cells with preserved axons), and weakly adapting spike responses (n = 8; data not shown). Most L2 GAD65-eGFP cells in the aPC also displayed basal dendrites. L2 GAD65-eGFP cells also differed markedly from glutamatergic SP cells in key intrinsic electrical and synaptic properties (see complete list in Table 1). For example, L2 GAD65-eGFP cells (n = 10) displayed much smaller and faster-decaying monosynaptic EPSCs evoked by LOT stimuli (Fig. 5B, C) as compared to SP cells (n = 16) at similar stimulus intensities (mean intensities = 46 and 40 μA, respectively, for L2 GAD65-eGFP and SP cells). The small monosynaptic EPSC in L2 GAD65-eGFP cells also differs from semilunar cells in L2, which have even larger such EPSCs than SP cells (Suzuki and Bekkers, 2011). In addition, the EPSCs in L2 GAD65-eGFP (n = 6) displayed a distinct dependence on stimulus number as compared to SP cells (n = 8) during 20-Hz LOT trains applied to LOT (100 μA; Fig. 5D). In biochemical analyses, a moderate number (31%) of GFP-positive cells co-labeled with antisense probes for GAD65 and GAD67 mRNA (n = 63; Fig. 5E), consistent with a GABAergic chemotype. In contrast, probes for VGLUTs, which

effectively labeled most cells in L2, did not co-label GFP-positive cells to any significant degree (3% for VGLUT1, $n = 545$; 0% for VGLUT2, $n = 35$). Thus, although many L2 GAD65-eGFP cells did not express detectable levels of GAD mRNA, L2 GAD65-eGFP cells without GAD are unlikely to be glutamatergic. This conclusion also fits with the physiological differences between L2 GAD65-eGFP cells and SP/semilunar cells.

Subjecting L2 GAD65-eGFP cells to variable LOT stimuli, we found that they, like SP cells, displayed a consistent, limited number of spikes per stimulus. The number of evoked spikes ranged between 1 and 2, as long as spikes were evoked, for both variable intensity single shocks (Fig. 6A, B) as well as 20-Hz stimulus trains (Fig. 6C, D; $n = 5$). In addition, as with SP cells, the consistent low number of spikes in L2 GAD65-eGFP cells appeared to be due to a component of gabazine-sensitive (10 μM; $n = 4$) inhibition with a relatively long onset delay (≥7 ms) that matched the spike-time in L2 GAD65-eGFP cells (Fig. 6E–G; no significant differences in all comparisons at given stimulus intensities or stimulus numbers). Furthermore, as expected if well-timed inhibition limited excitation, gabazine (10 μM) greatly increased spike number in response to variable-intensity single-stimulus pulses (Fig. 6B, $n = 3$) as well as 20-Hz stimulus trains (Fig. 6D, $n = 4$).

L3 FS cells provide the inhibition that limits spike number across a range of stimulus conditions

A final question that we addressed was what cell-type provided the inhibition that limited the spike response across stimulus conditions. We hypothesized that a likely candidate was a population of interneurons in layer 3, L3 fast-spiking (FS) cells, based on the relatively long onset-time to the IPSCs that we recorded in SP cells (≥7 ms; see Fig. 2B). Both L3 FS cells and GABAergic interneurons in L1 can provide inhibition onto SP cells (Stokes and Isaacson, 2010; Suzuki and Bekkers, 2012), but inhibition from L3 FS cells has a longer onset-time, reflecting the more complex feedback path leading to its generation. Inhibition from L3 FS cells should also impact spike activity of SP cells since it is targeted at or near the cell bodies of SP cells (Stokes and Isaacson, 2010; Suzuki and Bekkers, 2010b, 2012).

Supporting a mechanism in which L3 FS cells limited spike activity in SP cells, we found that the onset-times for IPSCs in SP cells were consistently well-matched with spikes in L3 FS cells ($n = 5$) when LOT stimulus intensity was varied (Fig. 7A, B; see *Experimental procedures* Section ‘Cell identification’ for method of identifying L3 FS cells). The IPSC and spike delays were both quite long (20–30 ms) at the lowest stimulus intensities but shortened to near 10 ms at higher intensities. Such a match was not observed in the onset delays of the IPSCs and spikes in interneurons in L1a ($n = 5$) or L1b ($n = 7$), which were near 5 ms at all intensities (Fig. 7A, B). Spiking in L3 FS cells ($n = 5$), but not interneurons in L1a ($n = 5$) or L1b ($n = 7$), also displayed changes in probability during 20-Hz stimulus trains that matched the time-course of IPSC probability in SP cells ($n = 6$; Fig. 7C, D). At the moderate stimulus intensities used in these experiments (30–80 μA; see *Methods*), the probability of spiking in L3 FS cells and the IPSC in SP cells both increased between pulses 1 and 2, then decreased across later pulses. The IPSC probabilities across these stimulus trains could have been affected by changes in transmitter release probability from the presynaptic cell, as well as that cell’s spike probability; nevertheless, the close match

between the spikes and IPSCs during the train is consistent with L3 FS cells providing inhibition onto SP cells. Interestingly, in the analysis across stimulus intensity (Fig. 7B), we found that spikes in not only L3 FS cells but also those in L2 GAD65-eGFP cells were closely matched in time to IPSCs in SP cells. Thus, we cannot exclude the possibility that L2 GAD65-eGFP cells also contributed a component of inhibition that limited SP cell spiking.

DISCUSSION

Input-spike coupling across stimulus conditions

Prior studies have shown that somatic inhibition can significantly impact the spike response of pyramidal cells in the aPC, limiting the number of spikes evoked by incoming inputs from mitral cells to near one spike per stimulus pulse (Tseng and Haberly, 1988; Luna and Schoppa, 2008). This effect occurs because the inhibition arrives with some delay following activation of mitral cell axons, which permits spikes but only a small number. Here, we have provided evidence that this mechanism is a general feature of the response of SP cells, occurring across a range of stimulus conditions relevant to the natural situation. In responses to both variable intensity LOT stimuli and variable stimulus patterns, we found that each stimulus pulse produced 1–2 spikes, when spiking occurred at all. Moreover, a factor that appeared to be very important in limiting spike number was the fact that somatic inhibition consistently tracked the timing of spikes across stimulus conditions; this naturally limited spike number to be near one if spiking occurred at all. We also found a scaling in the amplitude of synaptic inhibition and excitation across stimulus intensity and during stimulus trains. Such amplitude scaling is similar to observations previously made for recurrent excitation versus feedback inhibition upon optogenetic excitation of pyramidal cells (Franks et al., 2011). In our studies, the observed scaling was between inhibition and a mixed excitatory response that included both monosynaptic signals derived from mitral cell axons as well as recurrent excitation initiated by LOT stimulation.

Besides providing evidence that a low spike number was a consistent feature of the SP cell response, our study also indicated that such behavior was not restricted to SP cells. In recordings performed in a population of interneurons in L2 labeled in GAD65-eGFP mice (L2 GAD65-eGFP cells), we found that well-timed inhibition limited responses to LOT stimulation to 1–2 spikes per stimulus across variable stimulus conditions. One caveat with these studies was that we were unable to demonstrate that all L2 GAD65-eGFP cells were GABAergic, as only 31% of these cells labeled with *in situ* probes for GAD65/67.

Contribution of feedback inhibition

One factor that likely contributed to the ability of somatic inhibition to limit spike number in aPC cells across stimulus conditions was its basic underlying mechanism. Across variable stimulus conditions, we found that IPSCs in SP cells were time-locked to spikes in L3 FS cells, a class of interneurons previously shown to be capable of mediating feedback inhibition onto SP cells (Stokes and Isaacson, 2010; Suzuki and Bekkers, 2012). A feedback path of inhibition, which involves prior activation of SP cells (Stokes and Isaacson, 2010), likely accounted for the observation that inhibition consistently tracked the timing of the

first spikes in SP cells, which, as discussed above, was important for limiting spike number. Such tracking would not have necessarily been predicted if somatic inhibition were mediated by a feedforward path that does not involve prior activation of SP cells.

Suzuki and Bekkers (2012) had a somewhat different interpretation of feedback inhibition from ours, suggesting that it involves activation of L3 FS cells by semilunar cells rather than SP cells. This was based in part on the fact that semilunar cells receive more direct mitral cell input than SP cells, which should make them more excitable; also, their feedback IPSCs were less delayed than SP cell spikes. We found in our cell-attached recordings that intact SP cells in fact could be quite readily excited by LOT stimulation – the perithreshold LOT stimulus intensity for SP cell spiking (mean = 57 μA; see above) was similar to that of the feedback IPSCs (mean = 58 ± 5 μA, n = 18) – while recordings of the feedback IPSCs indicated that their onset times were quite similar to SP cell spikes. We thus propose that SP cells provide a significant source of excitation for L3 FS cells (Stokes and Isaacson, 2010).

Our results also appear to differ from prior studies (Stokes and Isaacson, 2010; Suzuki and Bekkers, 2012) in that we found little evidence for feedforward inhibition derived from L1 interneurons. Fast-onset inhibition with onset delays of 3–4 ms, consistent with feedforward path, was observed occasionally, but the more typical inhibitory response had delays of at least 7 ms. Moreover, the onset delays of the IPSCs closely tracked the spike times in L3 FS cells but not L1 interneurons (Fig. 7). Why we did not consistently observe feedforward inhibition in our recordings is not clear, although one possibility is that it reflected our animal model (GFP65-eGFP mice versus GAD67-GFP mice for Suzuki and Bekkers and rats for Stokes and Isaacson).

Functional implications

While care must be taken in interpreting our brain slice experiments in an *in vivo* context, our analysis of the L2 cell responses across a range of LOT stimulus intensities could be relevant to the natural situation in which odor concentration varies. With increasing concentration, odors typically increase both the number of activated glomeruli (Rubin and Katz, 1999; Meister and Bonhoeffler, 2001), as well as the number of activated mitral cells (Bathellier et al., 2008), either of which would likely result in greater input onto SP cells. Our observation that SP cells maintain a near-constant 1–2 spikes per stimulus at different LOT intensities suggests that inhibition could help limit the SP cell response across odor concentration. It is important to point out that SP cell responses were not completely invariant across LOT stimulus intensities. There were differences in both spike probability and timing (Fig. 1B, C), factors that would allow information about differences in odor concentration to be transmitted to the cortex.

The value of having a limited number of spikes itself may be related to the nature of mitral cell input into cortex. Individual mitral cells engage in prolonged spike bursts during bouts of inhalation (Margrie and Schaefer, 2003; Cury and Uchida, 2010), while groups of mitral cells engage in synchronized oscillations at the beta or gamma frequency pattern (Adrian, 1950; Kashiwadani et al., 1999; Neville and Haberly, 2003; Martin et al., 2004; Beshel et al., 2007). If an SP cell responds with only 1–2 spikes for each round of input, it is more likely to respond faithfully to subsequent inputs. Such coupling may be important for

maintaining any temporal coding feature present in beta/gamma oscillations (Laurent et al., 2001; Schaefer et al., 2006; Lepousez and Lledo, 2013) or for allowing the cortex to engage in its own oscillations (Freeman, 1959) that are coherent with those in the bulb (Bressler, 1984; Neville and Haberly, 2003).

Conclusions

In this study, we have identified circuit features of the piriform cortex that help ensure a short-duration excitatory response in cortical cells across a wide range of stimulus conditions. These include a prominent component of somatic inhibition derived from GABAergic cells in layer 3 that is well-timed with respect to pyramidal cell excitation. The limited excitation in response to a single stimulus pulse likely would enhance the ability of the cortex to detect various known output properties of the olfactory bulb, including patterns of spikes and beta/gamma oscillations. Among the questions to be addressed with further studies is whether the identified mechanisms are in fact critical *in vivo.* Would silencing specific GABAergic cells disrupt odor-evoked cortical oscillations that may be driven by oscillatory bulbar inputs? Also, what impact would disrupting these detection mechanisms have on odor discrimination, which is significantly impacted by fast bulbar oscillations (Lepousez and Lledo, 2013)?

Acknowledgments

We thank Dr. Michael T. Shipley (University of Maryland) for sending us the GAD65-eGFP mice and Dr. Qian-Quan Sun (University of Wyoming) for assisting with preliminary experiments in GAD65-eGFP mice.

GRANTS

NIH grants F32 DC010313 (DCS), R01 DK078749 (STH), R01 DC006640 (NES), and P30 DC004657 to the Rocky Mountain Taste and Smell Center.

Abbreviations

aPC	anterior piriform cortex
DIG	digoxigenin
EGTA	ethylene glycol tetraacetic acid
EPSC/EPSP	excitatory post-synaptic current/potential
GAD67	glutamic acid decarboxylase 67
GAD65-eGFP	glutamic acid decarboxylase 65-enhanced green fluorescent protein
HEPES	4-(2-hydroxyethyl)-1-piperazineethanesulfonic acid
IPSC	inhibitory post-synaptic current
L1	L2, L3, layer 1, layer 2, layer 3
L3 FS cell	Layer 3 fast-spiking cell
LOT	lateral olfactory tract
SP cell	superficial pyramidal cell

VGLUT vesicular glutamate transporter

References

Adrian ED. The electrical activity of the mammalian olfactory bulb. Electroencephalogr Clin Neurophysiol. 1950; 2:377–388. [PubMed: 14793507]

Bathellier B, Buhl DL, Accolla R, Carleton A. Dynamic ensemble odor coding in the mammalian olfactory bulb: sensory information at different timescales. Neuron. 2008; 57:586–598. [PubMed: 18304487]

Bekkers JM, Suzuki N. Neurons and circuits for odor processing in the piriform cortex. Trends Neurosci. 2013; 36:429–438. [PubMed: 23648377]

Beshel J, Kopell N, Kay LM. Olfactory bulb gamma oscillations are enhanced with task demands. J Neurosci. 2007; 27:8358–8365. [PubMed: 17670982]

Bressler SL. Spatial organization of EEGs from olfactory bulb and cortex. Electroencephalogr Clin Neurophysiol. 1984; 57:270–276. [PubMed: 6199188]

Cury KM, Uchida N. Robust odor coding via inhalation-coupled transient activity in the mammalian olfactory bulb. Neuron. 2010; 68:570–585. [PubMed: 21040855]

Ekstrand JJ, Domroese ME, Feig SL, Illig KR, Haberly LB. Immunocytochemical analysis of basket cells in rat piriform cortex. J Comp Neurol. 2001; 434:308–328. [PubMed: 11331531]

Franks KM, Isaacson JS. Synapse-specific downregulation of NMDA receptors by early experience: a critical period for plasticity of sensory input to olfactory cortex. Neuron. 2005; 47:101–114. [PubMed: 15996551]

Franks KM, Russo MJ, Sosulski DL, Mulligan AA, Siegelbaum SA, Axel R. Recurrent circuitry dynamically shapes the activation of piriform cortex. Neuron. 2011; 72:49–56. [PubMed: 21982368]

Freeman WJ. Distribution in time and space of prepyriform electrical activity. J Neurophysiol. 1959; 22:644–645. [PubMed: 13824766]

Jarvie BC, Hentges ST. Expression of GABAergic and glutamatergic phenotypic markers in hypothalamic proopiomelanocortin neurons. J Comp Neurol. 2012; 520:3863–3876. [PubMed: 22522889]

Kashiwadani H, Sasaki YF, Uchida N, Mori K. Synchronized oscillatory discharges of mitral/tufted cells with different molecular receptive ranges in the rabbit olfactory bulb. J Neurophysiol. 1999; 82:1786–1792. [PubMed: 10515968]

Laurent G, Stopfer M, Friedrich RW, Rabinovich MI, Volkovskii A, Abarbanel HD. Odor encoding as an active, dynamical process: experiments, computation, and theory. Annu Rev Neurosci. 2001; 24:263–297. [PubMed: 11283312]

Lepousez G, Lledo PM. Odor discrimination requires proper olfactory fast oscillations in awake mice. Neuron. 2013; 80:1010–1024. [PubMed: 24139818]

Litaudon P, Garcia S, Buonviso N. Strong coupling between pyramidal cell activity and network oscillations in the olfactory cortex. Neuroscience. 2008; 156:781–787. [PubMed: 18790020]

Lopez-Bendito G, Sturgess K, Erdelyi F, Szabo G, Molnar Z, Paulsen O. Preferential origin and layer destination of GAD65-eGFP cortical interneurons. Cereb Cortex. 2004; 14:1122–1133. [PubMed: 15115742]

Luna VM, Schoppa NE. GABAergic circuits control input-spike coupling in the piriform cortex. J Neurosci. 2008; 28:8851–8859. [PubMed: 18753387]

Margrie TW, Schaefer AT. Theta oscillation coupled spike latencies yield computational vigour in a mammalian sensory system. J Physiol. 2003; 546:363–374. [PubMed: 12527724]

Martin C, Gervais R, Hugues E, Messaoudi B, Ravel N. Learning modulation of odor-induced oscillatory responses in the rat olfactory bulb: a correlate of odor recognition? J Neurosci. 2004; 24:389–397. [PubMed: 14724237]

Meister M, Bonhoeffler T. Tuning and topography in an odor map on the olfactory bulb. J Neurosci. 2001; 21:1351–1360. [PubMed: 11160406]

Neville KR, Haberly LB. Beta and gamma oscillations in the olfactory system of the urethane-anesthetized rat. J Neurophysiol. 2003; 90:3921–3930. [PubMed: 12917385]

Patterson MA, Lagier S, Carleton A. Odor representations in the olfactory bulb evolve after the first breath and persist as an odor afterimage. Proc Natl Acad Sci U S A. 2013; 110:E3340–E3349. [PubMed: 23918364]

Poo C, Isaacson JS. Odor representations in olfactory cortex: “sparse” coding, global inhibition, and oscillations. Neuron. 2009; 62:850–861. [PubMed: 19555653]

Pouille F, Scanziani M. Enforcement of temporal fidelity in pyramidal cells by somatic feed-forward inhibition. Science. 2001; 293:1159–1163. [PubMed: 11498596]

Rubin BD, Katz LC. Optical imaging of odorant representations in the mammalian olfactory bulb. Neuron. 1999; 23:499–511. [PubMed: 10433262]

Schaefer AT, Angelo K, Spors H, Margrie TW. Neuronal oscillations enhance stimulus discrimination by ensuring action potential precision. PLoS Biol. 2006; 4:e163. [PubMed: 16689623]

Schoppa NE, Kinzie JM, Sahara Y, Segerson TP, Westbrook GL. Dendrodentritic inhibition in the olfactory bulb is driven by NMDA receptors. J Neurosci. 1998; 18:6790–6802. [PubMed: 9712650]

Stokes CC, Isaacson JS. From dendrite to soma: dynamic routing of inhibition by complementary interneuron microcircuits in olfactory cortex. Neuron. 2010; 67:452–465. [PubMed: 20696382]

Suzuki N, Bekkers JM. Neural coding by two classes of principal cells in the mouse piriform cortex. J Neurosci. 2006; 26:11938–11947. [PubMed: 17108168]

Suzuki N, Bekkers JM. Inhibitory neurons in the anterior piriform cortex of the mouse: classification using molecular markers. J Comp Neurol. 2010a; 518:1670–1687. [PubMed: 20235162]

Suzuki N, Bekkers JM. Distinctive classes of GABAergic interneurons provide layer-specific phasic inhibition in the anterior piriform cortex. Cereb Cortex. 2010b; 20:2971–2984. [PubMed: 20457693]

Suzuki N, Bekkers JM. Two layers of synaptic processing by principle neurons in piriform cortex. J Neurosci. 2011; 31:2156–2166. [PubMed: 21307252]

Suzuki N, Bekkers JM. Microcircuits mediating feedforward and feedback synaptic inhibition in the piriform cortex. J Neurosci. 2012; 32:919–931. [PubMed: 22262890]

Tang AC, Hasselmo ME. Selective suppression of intrinsic but not afferent fiber synaptic transmission by baclofen in the piriform (olfactory) cortex. Brain Res. 1994; 659:75–81. [PubMed: 7820683]

Tseng GF, Haberly LB. Characterization of synaptically mediated fast and slow inhibitory processes in piriform cortex in an in vitro slice preparation. J Neurophysiol. 1988; 59:1352–1376. [PubMed: 3385464]

Whitesell JD, Sorensen KA, Jarvie BC, Hentges ST, Schoppa NE. Interglomerular lateral inhibition targeted on external tufted cells in the olfactory bulb. J Neurosci. 2013; 33:1552–1563. [PubMed: 23345229]

Young A, Sun Q-Q. GABAergic inhibitory interneurons in the posterior piriform cortex of the GAD67-GFP mouse. Cereb Cortex. 2009; 19:3011–3029. [PubMed: 19359350]

Zhang C, Szabo G, Erdelyi F, Rose JD, Sun Q-Q. Novel interneuronal network in the mouse posterior piriform cortex. J Comp Neurol. 2006; 499:1000–1015. [PubMed: 17072835]

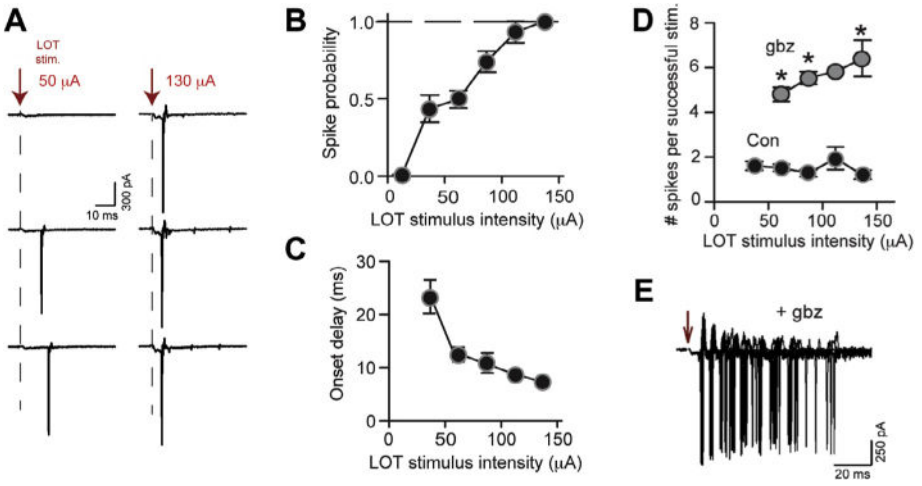

Fig. 1.

SP cells display 1–2 spikes across LOT stimulus intensities. (A) Cell-attached recordings of spike activity in an SP cell. Responses are shown to low-to-moderate intensity stimuli (50 μA) that were perithreshold for generation of spikes and, also, to much higher intensity stimuli (130 μA). Stronger stimuli elicited spikes more consistently, but the number of evoked spikes when there were spikes remained constant, at one. (B, C) Increasing LOT stimulus intensity resulted in a higher probability of spiking (B) and much shorter spike onset-delays to the first spike (C). This indicated that the stimulus intensities sampled resulted in large differences in the network behavior. Stimulus intensities were grouped into 25-μA bins centered on the indicated values on the *x*-axes. *N* values for each data point ranged from 4 to 13. Error bars were smaller than the symbols in some cases. (D) The mean number of spikes evoked in SP cells during successful trials (when spikes were evoked) was invariant ranging between 1 and 2 across stimulus intensity. Gabazine (10 μM; gbz) increased the number of evoked spikes. (E) An example recording in gabazine (60-μA stimulus intensity; three superimposed trials).

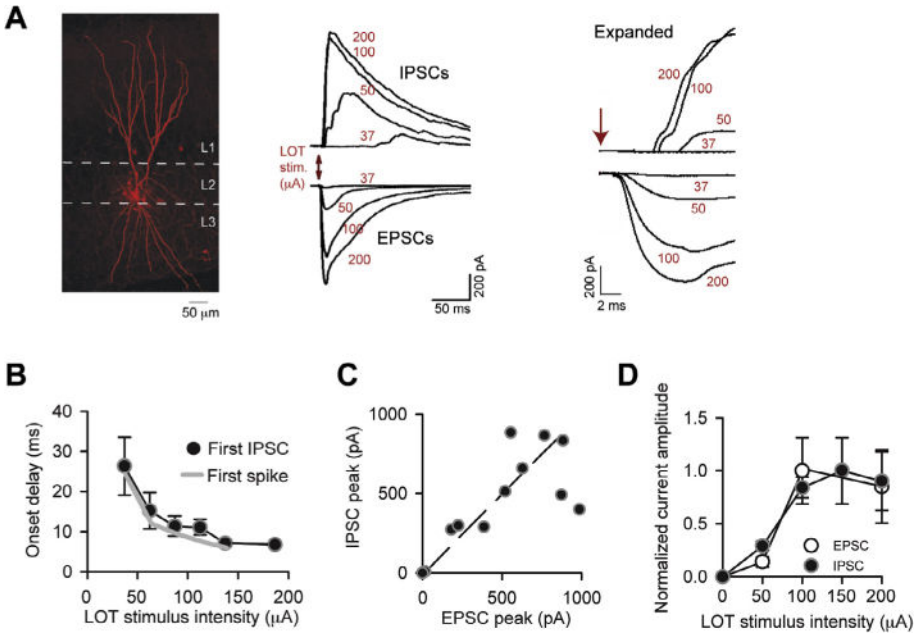

Fig. 2.

Inhibition is well-matched to excitation across LOT stimulus intensities. (A) IPSCs and EPSCs recorded in an SP cell in response to LOT stimulation at different intensities (indicated in red). IPSCs and EPSCs were recorded, respectively, at V_{hold} = −7 and −77 mV. In the expanded traces at right, monosynaptic EPSCs with short onset delays can be observed, while the onset delays of the IPSCs were longer. Traces reflect single trials. The EPSCs evoked by higher intensity stimuli likely included both monosynaptic and recurrent excitation. (B) The onset delays for the first spike were well-matched to the first IPSC in SP cells across LOT stimulus intensities. Spike onset delays (gray curve) reflect same data as in Fig. 1C. Data came from parallel recordings made in cell-attached (spikes) or whole-cell (IPSCs) modes. *N* values for each point for the IPSC data ranged from 3 to 20. (C) Inhibition scales in amplitude with excitation in SP cells. Each data point reflects peak EPSC and IPSC amplitude measurements made in a single cell at one stimulus intensity, averaged across ≥ 5 trials; data were pooled from seven recordings. Diagonal line reflects unity. (D) Average EPSC and IPSC amplitudes as a function of stimulus intensity, normalized to the peak current evoked by any stimulus in each recording. Stimulus intensities were grouped into 50-μA bins centered at the indicated values on the *x*-axis. *N* values for each data point ranged from 3 to 43. (For interpretation of the references to color in this figure legend, the reader is referred to the web version of this article.)

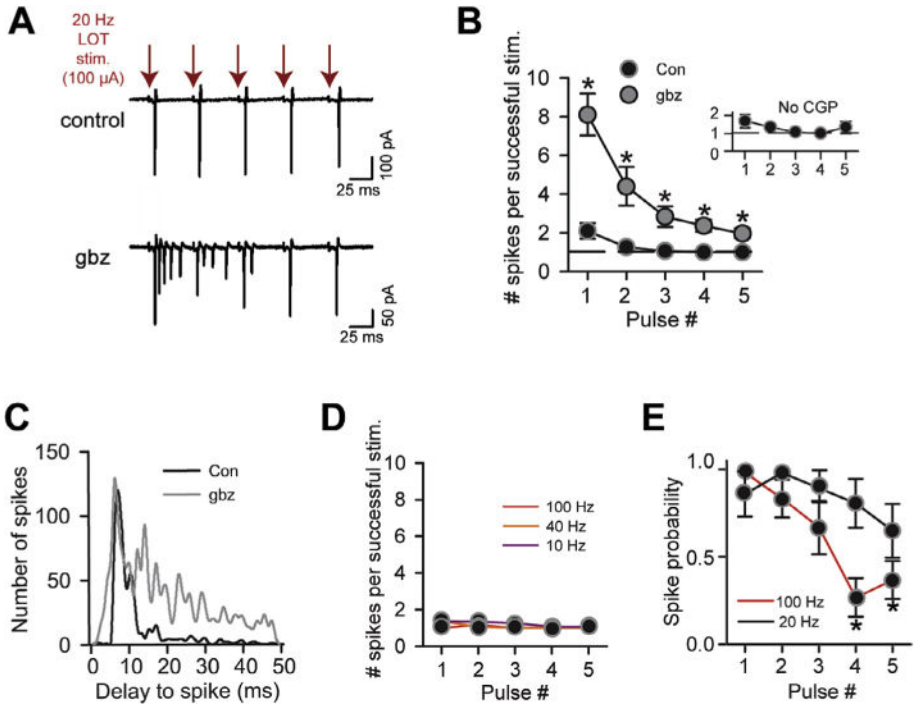

Fig. 3.

SP cells consistently display 1–2 spikes per stimulus during LOT stimulus trains. (A) Spike activity recorded in the cell-attached mode in an SP cell in response to five pulses of a 20-Hz stimulus train applied to LOT (100 µA). Under control conditions (top), the cells responded to each stimulus with a single spike. Gabazine (bottom) greatly increased the number of evoked spikes across the stimulus train. (B) The mean number of evoked spikes in successful trials (when spikes were evoked) as a function of stimulus number during a 20-Hz train. Asterisks denote significant differences ($p < 0.05$) for the gabazine data versus control. LOT stimulus intensity was 100 µA for all recordings. Inset reflects recordings in a bath solution that lacked the $GABA_B$ receptor antagonist CGP55845 ($n = 6$), different from our standard bath solution. (C) The onset-delay of spiking (all spikes) was quite consistent across the 20-Hz stimulus train under control conditions, but spikes were much more dispersed in gabazine. Histograms reflect pooled data from 5 to 7 recordings. All data were obtained using 100-µA LOT stimuli. (D) Stimulus patterns at 10, 40, and 100 Hz also produced a consistent spike number that varied between 1 and 2. For all data points ($n = 5$), error bars were smaller than the symbols. (E) The probability of spiking did not significantly change across the five stimuli for the 20-Hz pattern, but dropped off at 100 Hz (pulses 4 and 5 compared to pulse 1).

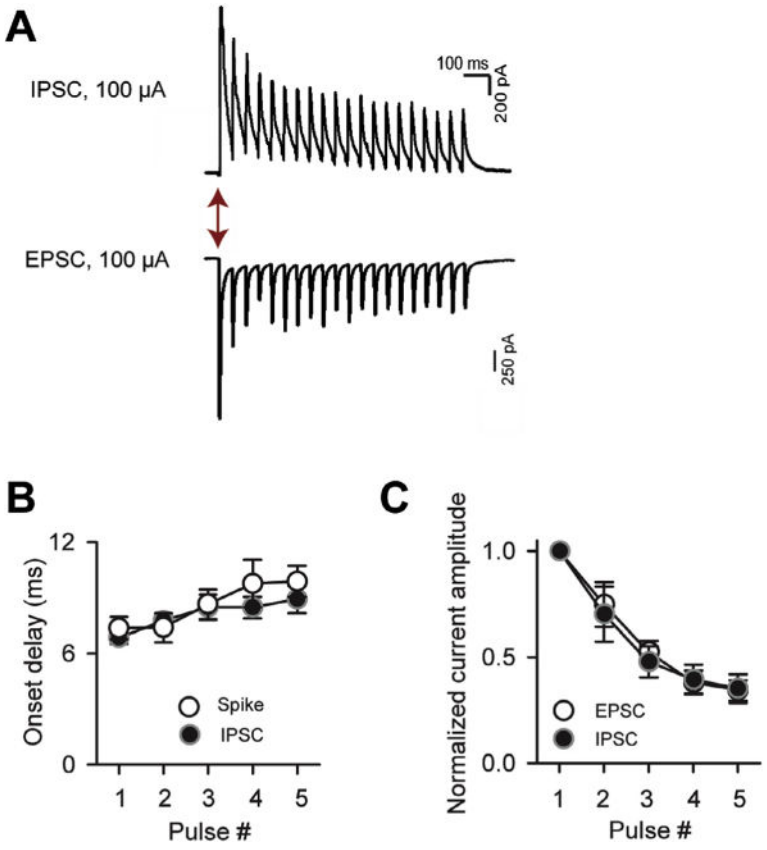

Fig. 4.

Inhibition is well-matched to excitation in SP cells across LOT stimulus trains. (A) IPSCs and EPSCs recorded in response to 20 Hz stimulus trains (20 pulses; 100-μA intensity). IPSCs and EPSCs were recorded, respectively, at V_{hold} = −7 and −77 mV. (B) The onset delays of the IPSCs (first-events) were well-matched to the spikes in SP cells across the first five pulses of the stimulus train. (C) EPSC and IPSC amplitudes as a function of stimulus number. Current values for each recording were normalized to the peak current evoked by any of the five stimuli. Note that both the EPSCs and IPSCs strongly depressed, but the currents remain well-matched in relative amplitude.

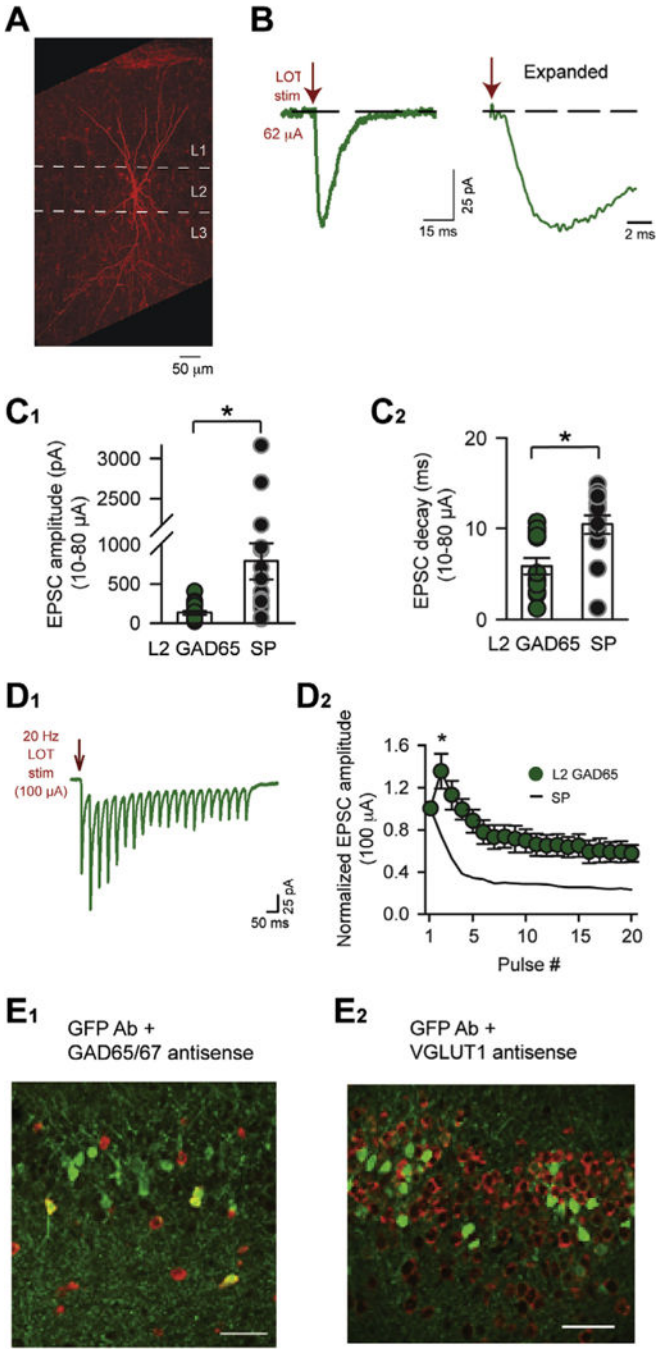

Fig. 5.

Characterization of L2 GAD65-eGFP cells. (A) An example biocytin-filled L2 GAD65-eGFP cell, showing a bitufted morphology with apical dendrites that extended high into L1 and basal dendrites. This cell also displayed an axon extending into L3. (B) Electrical stimulation of LOT induced monosynaptic EPSCs in an L2 GAD65-eGFP cell (average of 10 trials; V_{hold} = −77 mV). The fast onset-time of the EPSCs (1–2 ms) is clear in the expanded trace at right. (C) Summary of monosynaptic EPSC amplitude (C_1) and decay (C_2) in L2 GAD65-eGFP cells and SP cells following weak-to-moderate LOT stimuli (10–80

μA). Note the large differences in the EPSCs between cell-types, especially in amplitude. (D) L2 GAD65-eGFP cells and SP cells could be further differentiated based on their responses to 20-Hz LOT stimuli (100 μA). The evoked EPSCs in L2 GAD65-eGFP cells (raw traces in D_1; summary in D_2) displayed an initial facilitation, followed by depression, whereas EPSCs in SP cells were purely depressing at this stimulus intensity (black trace, same data as in Fig. 4C). Asterisk at pulse 2 indicates significant differences in the normalized EPSC values between L2 GAD65 eGFP and SP cells. (E) *In situ* hybridization and immunodetection of GFP. E_1: Several GFP-positive cells (green) co-labeled with anti-sense probes for GAD (red; combination of probes for both GAD65 and 67). E_2: In contrast, no GFP-positive cells co-labeled with an anti-sense probe for the vesicular glutamate transporter 1 (VGLUT1; in red).

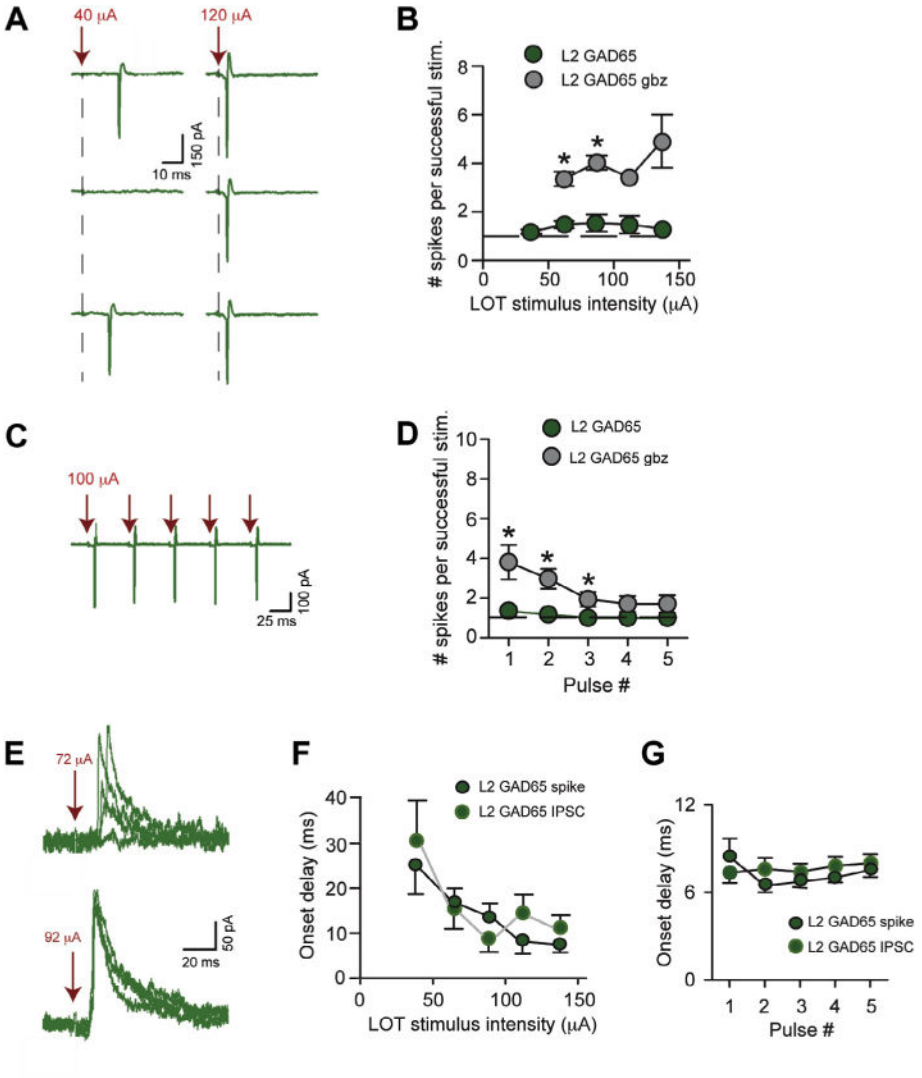

Fig. 6.

Well-timed inhibition limits the spike response of L2 GAD65-eGFP cells. (A) Cell-attached recording of spike activity in an L2 GAD65-eGFP cell. Responses are shown to moderate intensity stimuli (40 μA) that were perithreshold for generation of spikes and, also, to high-intensity stimuli (120 μA). The number of evoked spikes when there were spikes remained constant, at one. (B) The mean number of spikes evoked during successful trials was invariant ranging between 1 and 2 across LOT stimulus intensity. Gabazine (10 μM; gbz) increased the number of evoked spikes. *N* values for control data points ranged between 4 and 17. (C) Spike activity recorded in an L2 GAD65-eGFP cell in response to a 20-Hz stimulus train applied to LOT (100 μA). (D) The mean number of evoked spikes during successful trials as a function of stimulus number during a 20-Hz train in L2 GAD65-eGFP cells. LOT stimulus intensity was 100 μA for all recordings. (E) Outward-going IPSCs (at V_{hold} = −7 mV) in an L2 GAD65-eGFP cell in response to LOT stimulation at two stimulus intensities. Five trials are shown for each intensity. (F) The onset delays for the first spike measured in cell-attached recordings were well-matched to the first IPSC across LOT

stimulus intensity. *N* values for each point ranged from 3 to 15. (G) The onset delays of the first IPSCs recorded in response to 20-Hz stimuli (raw data not shown) were well-matched to the first spikes in L2 GAD65-eGFP cells.

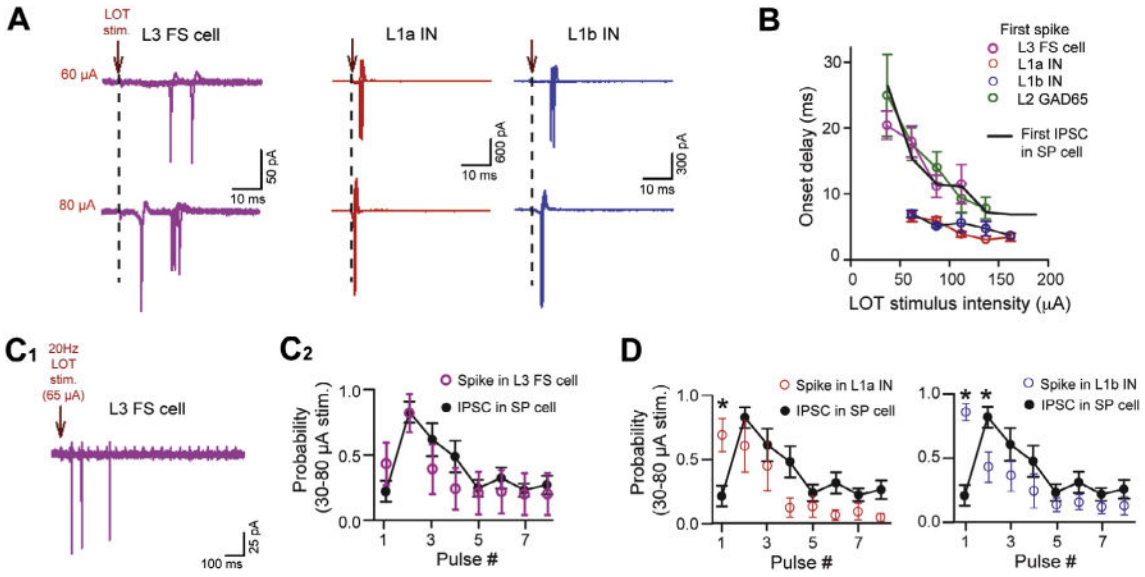

Fig. 7.

L3 fast-spiking (FS) cells mediate inhibition of L2 cells across variable LOT stimuli. (A) Example traces of spike activity recorded in cell-attached patches in an L3 FS cell (purple) and interneurons (INs) in L1a (red) and L1b (blue). Data are shown at moderate and higher stimulus intensities for each cell. (B) Summary. The onset delays to the first spikes in L3 FS cells, but not L1 INs, were well-matched to the first IPSCs in SP cells (black curve). The first spikes in L2 GAD65-eGFP cells were also matched to the IPSCs. The IPSC delays reflect the same data as in Fig. 2B; the spike data for L2 GAD65-eGFP cells reflect the plot in Fig. 6F. (C) Spiking in L3 FS cells during 20-Hz stimulus patterns was well-matched to the IPSCs in SP cells. Displayed are a sample trace of spike activity in an L3 FS cell (C_1) and summary (C_2) plotting the probability of L3 FS cell spiking or IPSC across the first eight stimuli. (D) Spike probabilities of INs in L1a (left) and L1b (right) were not well-matched to the IPSCs during 20-Hz stimulus trains.

Table 1

Intrinsic and excitatory synaptic properties of L2 GAD65-eGFP and SP cells. Intrinsic electrical properties examined included input resistance (R_i), resting potential (V_{rest}), half-width of action potential (AP width), and current step required to elicit spiking from rest ($I_{spiking}$). Measurements of excitatory post-synaptic currents (EPSCs) yielded estimates for the peak amplitude (Amp_{EPSC}), decay time-constant (τ_{EPSC}), and response characteristic during a 20-Hz stimulus train. EPSCs yielding estimates of Amp_{EPSC} and τ_{EPSC} were elicited by moderate-intensity stimuli applied to LOT (means of 46 and 40 μA, respectively, for L2 GAD65-eGFP and SP cells), when the EPSC should have mainly reflected monosynaptic transmission from LOT

	R_i (MΩ)	V_{rest} (mV)	AP width (ms)	$I_{spiking}$
Intrinsic electrical properties				
L2 GAD65-eGFP	195 ± 16 (*n* = 32)	−65 ± 1 (*n* = 28)	0.97 ± 01 (*n* = 14)	37 ± 6 pA (*n* = 14)
SP	111 ± 14 (*n* = 27)	−71 ± 1 (*n* = 31)	1.66 ± 0.01 (*n* = 15)	152 ± 37 (*n* = 5)
p-value	<0.001	<0.001	<0.001	0.003

	Amp_{EPSC} (pA)	τ_{EPSC} (ms)	20 Hz train (100 μA)
EPSCs evoked by LOT stimulation			
L2 GAD65-eGFP	−42 ± 3 (*n* = 10)	5.8 ± 0.9 (*n* = 10)	Facilitating-then-depressing (*n*=6)
SP	−173 ± 59 (*n* = 16)	10.4 ± 1.0 (*n* = 16)	Depressing (*n*=8)
p-value	0.036	0.003	